High power compact continuous-wave Fe:ZnSe laser at 4-μm with >50% overall conversion efficiency

Yanlong Shen (沈炎龙)*, Yingchao Wan(万颖超), Feng Zhu(朱 峰), Tongxing Chai(柴童星), Yousheng Wang(汪由胜), and Ke Huang(黄 珂)

State Key Laboratory of Laser Interaction with Matter, Northwest Institute of Nuclear Technology, Xi'an Shaanxi, 710024, China

*Corresponding author: yanlong_xian@126.com;

Received Month X, XXXX; accepted Month X, XXXX; posted online Month X, XXXX

We report on a compact, high efficiency mid-infrared continuous-wave (CW) Fe:ZnSe laser pumped by a 2.9 μm fiber laser under liquid nitrogen cooling. A maximum output power of 5.5 W and a slope efficiency of up to 66.3% with respect to the launched pump power were obtained. The overall optical-to-optical (OTO) conversion efficiency, calculated from the output of 2.9 μm fiber laser to the 4-μm laser, was as high as ~54.5%. The OTO efficiency and the slope efficiency are, to the best of our knowledge, the highest in ever reported Fe:ZnSe lasers. A rate-equation-based numerical model of CW operation was established, and the simulation agreed well with the experiment, identifying the routes used in the experiment for such high efficiency.

Keywords*:* Fe:ZnSe, mid-infrared laser, high efficiency, solid-state laser.

DOI: 10.3788/COLXXXXXX.XXXXXX.

1.Introduction

There are increasing demands for high power solid-state mid-infrared lasers at 3~5 μm, for their applications in laser radar, spectroscopy, remote sensing, infrared countermeasures, laser communication, etc[1-3]. Currently, the principal category of solid-state lasers at this band is based on the nonlinear effect, including optical parametric oscillators[4-5](OPOs, typically using PPLN and ZGP crystals as nonlinear media), difference frequency generation (DFG)[6], and frequency doubling[7]. Yet there are only a few direct solid-state mid-infrared 3~5 μm laser sources, merely including quantum cascade lasers[8-9], fiber lasers[10] and transition metal (TM) ions doped crystalline lasers (typically Fe:ZnSe or Fe:ZnS lasers)[1,11]. Compared with these lasers, Fe:ZnSe or Fe:ZnS lasers, emitting at the mid-infrared range of 4~5 μm, enjoy the impressive advantages of high efficiency, wide wavelength-tuning range, and compactness of optical cavity, etc[12]. As such, lots of efforts have been made in the development of Fe:ZnSe/Fe:ZnS lasers in the past decade. Since Fe:ZnSe crystal was demonstrated to be an effective gain medium for 4-μm lasers for the first time in 1999[1], lots of Fe:ZnSe lasers in different regimes, including CW[2], gain-switching[3], Q-switching[13-14], mode-locking[15] were demonstrated by employing various pumping sources at ~3 μm. For some practical applications, high power and highly stable CW 4-μm lasers are urgently required. The upper laser level lifetime of Fe^{2+} in ZnSe crystal is ~60 μs at 77 K while as short as ~370 ns at room temperature[16], as a consequence, it is necessary to cool Fe:ZnSe crystal down to ~77 K by liquid nitrogen in a cryostat for efficient CW operation. In 2008, Voronov reported the first operation of CW Fe:ZnSe laser pumped by a 2.97 μm Cr:CdSe laser[17], of which the maximum output power and an OTO efficiency (i.e., the laser output power to the power of pump source output end) were 160 mW and 27%, respectively. Subsequently, Evans et al demonstrated CW Fe:ZnSe lasers with output powers of 840 mW and 420 mW by using two Er:YAG lasers at 2.94 μm[2] and an Er:Y_2O_3 laser at 2.74 μm[18], and the corresponding OTO efficiencies were ~28% and 13.3%, respectively. Martyshkin et al developed a Cr:ZnSe laser at 2.94 μm with an output power of 23 W for power scaling. With the powerful pump source, they achieved a CW Fe:ZnSe laser with a maximum power of 9.2 W and an OTO efficiency of ~40%[19]. Recently, Li et al presented a CW Fe:ZnSe laser pumped by an Er:YAP laser[20], whose output power and OTO efficiency were ~1 W and 27.8%, respectively. Compared to solid-state pump lasers, fiber lasers possess the advantages of high beam quality and high stability, which are supposed to be ideal sources for pumping. Thanks to the dramatical development of fluoride fiber lasers at ~3 μm in the past decades[21-23], of which the recorded CW output power was as high as 41.6 W[23], therefore, it is natural to employ a fiber laser at ~3 μm to pump Fe:ZnSe crystals. In 2018, Pushkin et al demonstrated a compact CW Fe:ZnSe laser with a maximum power of 2.1 W and an OTO efficiency of 32% pumped by an Er:ZBLAN fiber laser at 2.8 μm[24]. Table 1 presents comparison of the state-of-the-art CW Fe:ZnSe lasers. The lack of high power CW pump source seems to be the main obstacle for 4-μm laser power scaling. However, promotion of OTO efficiency is more important for obtaining higher output power when pump power is limited.

Tab. 1 State-of-the-art CW Fe:ZnSe lasers

Pump source	Fe:ZnSe laser	η_s^a	η_o^b	Reference
Cr:CdSe laser(0.6 W at 2.97μm)	160 mW	<56%	26.7%	[17]
Two Er:YAG lasers (total 3 W at 2.94 μm)	840 mW	~40%	28%	[2]
Er:Y_2O_3 (3.15 W at 2.74 μm)	420 mW	17.3%	13.3%	[18]
Cr:ZnSe (23 W at 2.94 μm)	9.2 W	41.2%	40.0%	[19]
Er:ZBLAN laser (6.5 W at 2.8 μm)	2.1 W	<59%	32.3%	[24]
Er:YAP laser(3.6 W at 2.92 μm)	~1 W	<48.2%	27.8%	[20]
Fluoride fiber laser (10.1 W at 2.91 μm)	5.5W	66.3%	54.5%	This work

[a] Slope efficiency with respect to launched pump power

[b] OTO efficiency with respect to power from the pump output end

In this work, we report on a high power, high efficiency and low-complexity Fe:ZnSe laser by adopting series of innovation, including customization of a pair of special coatings into the Fe:ZnSe crystal working facets for lower cavity loss, and a longer wavelength pump source for higher pump absorption and higher quantum efficiency. The maximum output power of 5.5 W was obtained under liquid nitrogen cooling, which is the highest in fiber-laser-pumped Fe:ZnSe lasers. The overall OTO efficiency with respect to the pump source was as high as ~54.3%. The central wavelength was tuned from 3.96 to 4.15 μm by improving pump power. The laser was considerably compact and nearly alignment-free, which led to fairly high long-term stability.

2.Experiments

The output of our CW Fe:ZnSe laser was compared under two different pump schemes, i.e., forward pumping (FP) and backward pumping (BP). The experimental setup of BP scheme is schematically shown in Fig. 1.

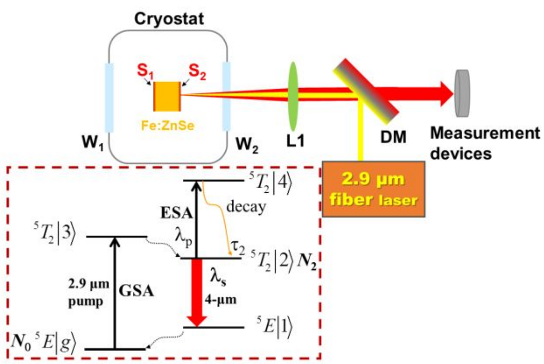

Fig. 1. Schematic layout of the 2.9 μm fiber-laser-pumped CW Fe:ZnSe laser of BP scheme. Inset: partial energy levels of Fe^{2+} ions involving pump absorption and laser emission.

Compared with the pump source of a 2.8 μm fiber laser in the previous demonstration[24], an all-fiber laser at 2.9-μm was developed to pump the Fe:ZnSe crystal in our experiment mainly based on the following considerations. One is that the longer wavelength of pump results in a promotion of the quantum efficiency compared to pumping at the shorter wavelengths, and the other is that the absorption cross-section at 2.9 μm of Fe:ZnSe at low temperature (LT) of ~77 K is larger than 2.8 μm[18]. In 2015, a maximum output power of 30.5 W was obtained from an Er:ZBLAN all-fiber laser at 2.94 μm[22], which was an ideal source for pumping Fe:ZnSe. As the techniques of writing fiber Bragg grating (FBG) in ZBLAN fiber and splicing between a ZBLAN fiber and a silica fiber continue to mature, it is common to develop an all-fiber laser at 3-μm waveband. A single-mode all-fiber CW Er:ZBLAN fiber laser with a maximum output power of ~10.1 W at a central wavelength of 2907.3 nm was in-house built to be used as the pump source. The pump beam was collimated with a collimator (f=12.7mm) and then focused into the Fe:ZnSe crystal through an uncoated CaF_2 lens (L1, f=50 mm). The pump beam waist diameter was measured to be around 400 μm. The Fe:ZnSe crystal, grown from the vapour phase by using a concurrent-doping technology[17], was a ~9 mm in length with a labeled Fe^{2+} ions concentration of 5.0×10^{18} cm^{-3}. The one-pass absorption coefficient was measured to be 5.14 cm^{-1} at a LT of ~77 K with a similar crystal with broadband AR coated for 2.7~4.8 μm. Consequently, the Fe^{2+} ions concentration was determined experimentally to be 5.5×10^{18} cm^{-3}, in which the absorption cross section at λ= 2907 nm (σ_{gsa}=0.94×10^{-18} cm^2) was taken from Ref[25].

For more compact cavity design, both working facets (7 mm×7 mm) of the crystal were polished carefully to reduce the residual wedge as far as possible. Two series of special coatings were deposited onto the polished facets. The coating of S1 (see Fig. 1) had a high transmittance at the pump wavelength (T≥95% at 2.6~3 μm) and a high reflectivity at the output wavelength (R>99% at 3.7~4.8 μm), while the coating of S2 had a high transmittance at the pump wavelength (T≥95% at 2.6~3 μm) and a partial transmittance at the output wavelength (R~65% at 3.7~4.8 μm), which served as the output coupler. The crystal was wrapped by a piece of indium foil and clamped to a U-shaped copper heat sink, and the temperature of the heat sink was controlled by a liquid-nitrogen-cooled cryostat from ~77 to ~300 K to study the influence of crystal temperature to the laser conversion efficiency. Inset of Fig. 1 is the partial energy levels of Fe^{2+} ions. The lifetime of upper laser level $^5T_2|2>$ reduces significantly when temperature of Fe:ZnSe crystal higher than 120 K due to the increase of the rate of non-radiative relaxation[26, 27]. Theoretically, longer lifetime of upper laser level makes CW emission much easier. Therefore, almost all the CW Fe:ZnSe lasers operated by cooling Fe:ZnSe crystals to low temperature, e.g., 77 K. The vacuum windows (W1 and W2) of the cryostat were 3 mm CaF_2 plates with broadband anti-reflection (AR, T~99%) coated for 2.7~4.8 μm. A dichroic mirror (DM, HR>99 % at 2.6~3 μm, HT>95% at 3.7~4.8 μm) was placed with an incidence angle of 45° to separate the pump beam and output laser beam. Forward pumping was carried out by just turning around the cryostat in Fig. 1.

3.Results and discussion

Firstly, output characteristics of the Fe:ZnSe laser were compared under different pumping schemes at a LT of ~77 K. The laser cavity was self-aligned and had a relatively low loss by customizing special coatings into the facets of the Fe:ZnSe crystal. It was easy to obtain the 4-μm laser output without any tedious alignment of the laser cavity in both schemes when the launched pump power was higher than the threshold of around 0.4 W. The output powers of FP and BP as a function of launched pump power were shown in Fig. 2. The maximum powers of FP and BP were 5.3 and 5.5 W at the full pump power of 10.1 W, respectively. The slope efficiencies were 61.9% in FP and as high as 66.3% in BP, corresponding to overall OTO efficiencies of 52.4% and 54.5%, respectively. Both the slope efficiency and the overall OTO efficiency are the highest in ever reported Fe:ZnSe lasers. The slope efficiency in BP was close to the limited laser efficiency, i.e., quantum efficiency (i.e., $\lambda_{pump}/\lambda_{laser}$), which is 69.9 % in our case. The results suggested that the performance of BP was slightly better than that of FP, which was similar to fiber lasers with different pump schemes[28]. The laser cavity length, i.e., the length of the crystal, was ~9 mm, which was nearly one order of magnitude shorter than previously reported Fe:ZnSe laser[3]. Such short cavity brought several advantages, including better cavity stability and lower cavity loss. In laser cavity design, an important parameter denoted Fresnel number can be expressed by $N=d^2/L\lambda$, where d is the diameter of excitation region in crystal and L is the cavity length. The shorter the cavity, the higher the Fresnel number, which in turn led to lower diffraction loss of cavity. The geometric loss was very small as well due to the high parallelism of cavity mirror. Thus, much lower cavity loss, through integrating the cavity mirrors and the crystal instead of cavity mirrors, was mainly responsible for such high efficiency. Further in this work, if not specially stated, our considerations are confined to the laser in BP regime. No thermal roll-off at the maximum pump power was observed, which indicated that further power scaling would be available by just increasing pump power. The output beam profile of BP at the maximum output power captured with a camera is shown in the inset of Fig. 3, from which we could found that the far-field beam spot had a symmetrical good Gaussian distribution. We measured the divergence of output beam in the forward pumping scheme with a CaF_2 lens (f=100 mm). The spot diameter at the focal plane was around 1.5 mm, therefore, the divergence was calculated to be 15 mrad (full angle).

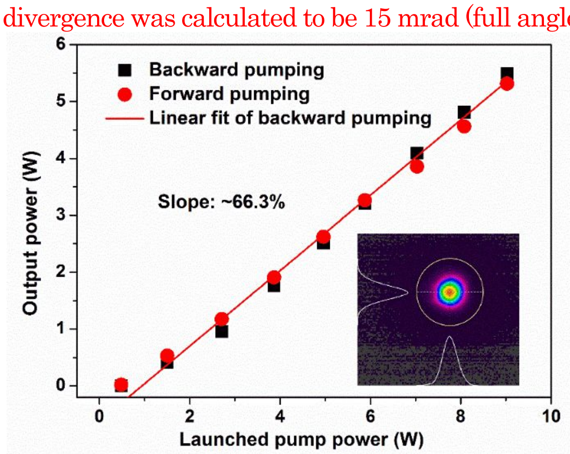

Fig. 2. Output powers of FP and BP as a function of launched pump power. Inset: the beam profiles of BP at the maximum output power.

The output spectra at various output powers were captured by a mid-infrared optical spectrum analyzer with a resolution as high as 0.2 nm, as typically shown in Fig. 3. The gain spectra of Fe:ZnSe at different temperatures are very broad, as shown in Fig. 4. The evolution trend of spectra was that the central wavelengths were red-shifted to longer positions with bandwidths broadened as increasing the pump power.

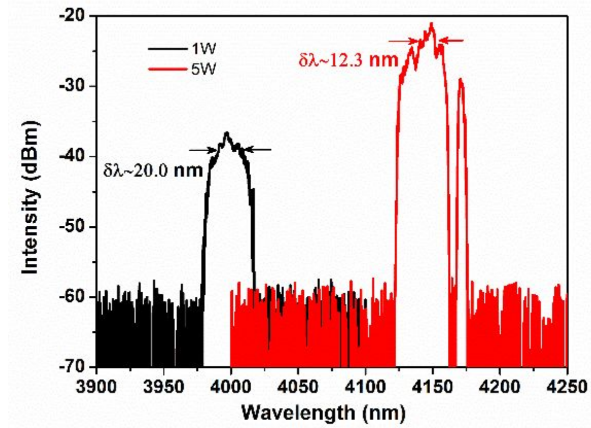

Fig. 3. Output spectra of Fe:ZnSe laser (BP) at low and high output powers.

The peak wavelength was 3.98 μm at the output power of ~1 W, and then shifted to 4.15 μm at ~5 W. The red-shift of central wavelength at different pump power is very common in free-running solid-state lasers, which is interpreted as increase of temperature of pumping region by local heating of gain crystal. A model was established to estimate the temperature distribution in the pumping area, and the highest temperatures generated in the center of pump beam spot were ~82.5 K at the output power of ~1 W and ~96.1 K at ~5 W, respectively. The increase of temperature was supposed to be responsible for such wavelength shift. There was a dip in the spectrum at the output power of 5W, the cause of which was attributed to the absorption by atmospheric CO_2 in the path from the output chamber window to the optical spectrum analyzer when measuring the spectrum. Compared to the spectra of a spiky structure in previous reports, the spectra in our case had a relatively smooth curve. It is interesting that the curves had only one peak with a FHWM bandwidth (3 dB) of ~20 nm at a low output power, and the bandwidth was slightly narrower (~12.3 nm) at a high power. The signal-to-noise ratio (SNR) was measured to be roughly 25 dB for low powers, and it was nearly 40 dB at the output power of 5 W.

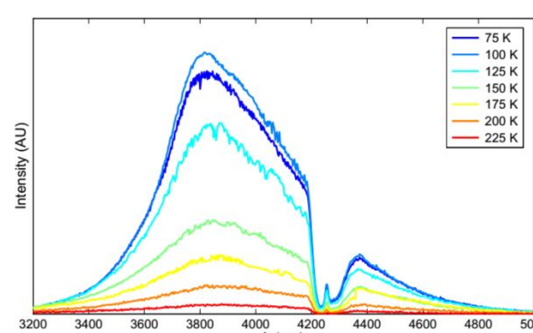

Fig. 4 Temperature-dependent gain spectra of Fe:ZnSe[29]

The laser output was fairly stable by integrating the cavity coatings into the crystal to avoid any possible factors causing instability. The long-term stability of the laser at an output power of over 5 W over a 1 h period was measured with a power meter, as shown in Fig. 5. The peak-to-peak fluctuation was calculated to be approximately 0.7% at nearly the maximum output power.

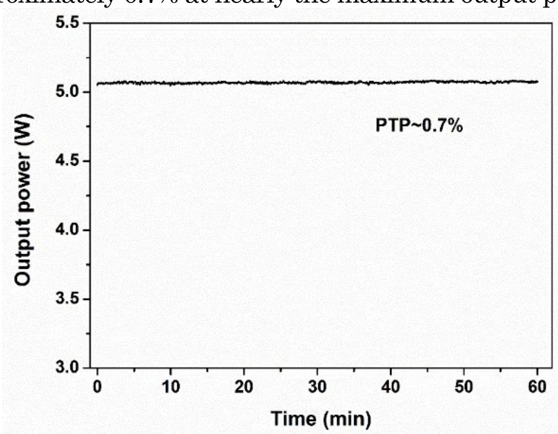

Fig. 5. The measured long-term stability at an output power of ~5 W in BP scheme over a 1 h period with a power meter with a response time of 0.6 s.

The conversion efficiency of our experiment was even higher than the previous simulation of CW operation[30], in which the slope efficiency at a LT of 77 K was only 42%. To gain insight into the laser dynamics and get an explanation for such high efficiency, we developed a numerical model of steady-state CW operation with rate-equation theory. Only the ground state ($^5E|g>$) and upper laser level ($^5T_2|2>$) of Fe^{2+} (see the inset of Fig. 1) need to be considered in the calculation. The ground state population and the upper laser level population were denoted as N_0 and N_2, respectively.

The power evolution of pump $P_p^{\pm}(z)$ and laser signal $P_s^{\pm}(z)$ (+ forwards, − backwards) along the cavity axis (with longitudinal coordinate z) could be expressed as follows:

$$\pm\frac{dP_p^{\pm}(z)}{dz}=-\sigma_{gsa}N_0(z)P_p^{\pm}(z)-\sigma_{esa}N_2(z)P_p^{\pm}(z)-\alpha_pP_p^{\pm}(z) \quad (1)$$

$$\pm\frac{dP_s^{\pm}(z)}{dz}=P_s^{\pm}(z)(g(z)-l)+P_{ASE} \quad (2)$$

where the gain $g(z)$ is:

$$g(z)=\Gamma\sigma_{se}N_2(z) \quad (3)$$

in Eq. (1)~(3), σ_{gsa}, σ_{esa} and σ_{se} are the ground absorption, excited-state absorption and emission cross sections of the Fe:ZnSe crystal, respectively; α_p is the intrinsic absorption coefficient of the crystal; Γ is the overlap coefficient of pump spot and laser spot; l is the total loss of the cavity including the intrinsic loss of crystal, geometry loss and diffraction loss. P_{ASE} is the power of amplified spontaneous emission (ASE), which is given by[31]:

$$P_{ASE}=\Gamma\frac{2hc^2}{\lambda_s^3}\sigma_{se}N_2(z)\Delta_{ASE} \quad (4)$$

where $\triangle_{ASE}$ is the ASE bandwidth centered at signal wavelength; h is the Planck constant; c is the speed of light in vacuum; λ_s is the laser wavelength.

$$\frac{dN_2(z,t)}{dt}=\frac{\lambda_p(P_p^+(z,t)+P_p^-(z,t))}{\pi r_p^2hc}(\sigma_{gsa}N_0(z,t)-\sigma_{esa}N_2(z,t))-\frac{\lambda_s(P_s^+(z,t)+P_s^-(z,t))}{\pi r_s^2hc}\sigma_{se}N_2(z,t)-\frac{N_2(z,t)}{\tau_f} \quad (5)$$

where λ_p is the pump wavelength, and τ_f is the fluorescence lifetime of upper laser level; r_p and r_s are the beam radii of pump and laser, respectively.

The output power of the Fe:ZnSe laser could be expressed by:

$$P_{out}=(1-R_2)P_s^+(L) \quad (6)$$

where R_2 is the reflectivity of output coupler, L is the position of output end of the cavity.

We carried out the model with parameters in line with our experiment, as shown in Tab. 2.

Tab. 2 Parameters of the Fe:ZnSe laser

Parameter	Value	Parameter	Value
σ_{gsa}	0.94×10^{-18}cm^{-2}[25]	τ_f	57 μs [27]
σ_{se}	1.1×10^{-18}cm^{-2}[25]	N_t	5×10^{18}cm^{-3}
$\sigma_{esa}/\sigma_{gsa}$	0.12[32]	Δ_{ASE}	1.13 μm[25]
l	variable	α_p	0.01 cm^{-1}
λ_p / λ_s	2.9 μm / 4.1 μm	n	2.4
R_1	0.99	R_2	0.65

The spectroscopic parameters of Fe^{2+} were taken from Ref[25]. According to Ref[32], the particles in upper laser level ($^5T_2|2>$) jump to the higher level via excited-state absorption process by absorbing the pump photons not the laser photons, which is different from the process of the simulation in Ref[30]. The ratio of σ_{esa} to σ_{gsa} was deduced to be 0.12 in terms of the experiment results in ReF[32]. The simulation of output power with these input conditions under various cavity losses was shown in Fig. 6. The slope efficiency decreased as increasing the total loss. The maximum slope efficiency was 63.1%, which was very close to our experimental result. That is, the cavity loss in our case was slightly lower than 0.05 cm^{-1} due to such compact cavity with a length of ~1 cm. The geometry loss and diffraction loss would be increased when the cavity length was lengthened by at least one order of magnitude in previous demonstrations[18-20]. Therefore, reducing the loss as much as possible is beneficial for high conversion efficiency.

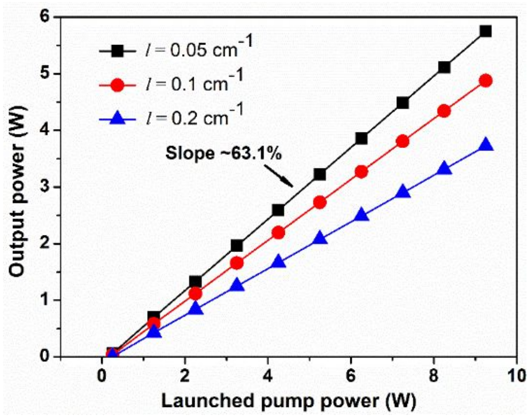

Fig. 6. The calculated output power as a function of launched pump power.

4.Conclusion

In conclusion, a high power, high efficiency fiber-laser-pumped all-solid-state CW Fe:ZnSe laser with a current-recorded overall efficiency as high as 54.5% is demonstrated. Output power of over 5 W with a central wavelength of around 4.1 μm was obtained from a Fe:ZnSe crystal under liquid nitrogen cooling. A numerical model was established to analyze factors of influencing high efficiency CW operation. The simulation was in line with our experiment, indicating that, output power scaling to tens of watts or even higher could be possible by employ this configuration just by using higher pump power.

This work was supported by the Fund of the State Key Laboratory of Laser Interaction with Matter (SKLLIM1912).

The authors are very grateful to Kunpeng Luan and Mengmeng Tao from the SKLLIM for fruitful discussions.

References

1. J. J. Adams, C. Bibeau, R. H. Page, D. M. Krol, L. H. Furu, and S. A. Payne, "4.0-4.5- μm lasing of Fe: ZnSe below 180 K, a new mid-infrared laser material," Opt. Lett. **24**(23), 1720-1720(1999).
2. J. W. Evans, P. A. Berry, K. L. Schepler, "840 mW continuous-wave Fe:ZnSe laser operating at 4140 nm," Opt. Lett. **37**(23), 5021-5023 (2012).
3. J. Kernal, V. V. Fedorov, A. Gallian, S. B. Mirov and V. V. Badikov, "3.9–4.8 μm gain-switched lasing of Fe:ZnSe at room temperature," Opt. Express **13**(26), 10608-10615(2005).
4. T. Xing, L. Wang, S. Hu, T. Cheng, X. Wu, and H. Jiang, "Widely tunable and narrow-bandwidth pulsed mid-IR PPMgLN-OPO by self-seeding dual etalon-coupled cavities," Opt. Express **25**(25), 31810-31815(2017).
5. G. Liu, S. Mi, K.Yang, D. Wei, J. Li, B. Yao, C. Yang, T. Dai, X. Duan, L. Tian, and Y. Ju, "161 W middle infrared $ZnGeP_2$ MOPA system pumped by 300 W-class Ho:YAG MOPA system," Opt. Lett. **46**(1), 82-85(2021).
6. C. Bao, Z. Yuan, H. Wang, L. Wu, B. Shen, K. Sung, S. Leifer, Q. Lin, and K. Vahala, "Mid-infrared frequency comb with 6.7 W average power based on difference frequency generation," Optica **7**(4), 309-315(2020).
7. L.P. Gonzalez, D. C. Upchurch, P. G. Schunemann, L. Mohnkern, and S. Guha, "Second-harmonic generation of a tunable continuous-wave CO_2 laser in orientation-patterned GaAs," Opt. Lett. **38**(3), 320-322(2013).
8. J. Faist, F. Capasso, D. L. Sivco, A.L. Hutchinson, C. Sirtori, and A.Y. Cho, "Quantum cascade laser A new optical source in the mid-infrared," Infrared Phys. Technol. **36**(1), 99-103(1995).
9. P. Täschler , M. Bertrand, B. Schneider , M. Singleton, P. Jouy, F. Kapsalidis , M. Beck and J. Faist, "Femtosecond pulses from a mid-infrared quantum cascade laser," Nature Photon. **15**, 919–924(2021).
10. F. Maes, V. Fortin, S. Poulain, M. Poulain, J.Y. Carree, M. Bernier, and R. Vallee, "Room-temperature fiber laser at 3.92 μm," Optica **5**(7), 761-764 (2018).
11. M. P. Frolov, Y. V. Korostelin, V. I. Kozlovsky, Y. P. Podmar'kov, S. A. Savinova, and Y. K. Skasyrsky, "3J pulsed Fe:ZnS laser tunable from 3.44 to 4.19μm," Laser Phys. Lett. **12**, 055001(2015).
12. S. B. Mirov, V. V. Fedorov, D. Martyshkin, I.S. Moskalev, M. Mirov, and S. Vasilyev, "Progress in Mid-IR Lasers Based on Cr and Fe-Doped II–VI Chalcogenides," IEEE J. Sel. Top. Quantum Electron. **21**(1), 1601719(2015).
13. J. W. Evans, P. A. Berry, and K. L. Schepler, "A passively Q-switched, CW-pumped Fe:ZnSe laser," IEEE J. Quantum Electron. **50**(3): 204-209(2014).
14. H. Uehara, T. Tsunai, B. Han, K. Goya, R. Yasuhara, F. Potemkin, J. Kawanaka, and S. Tokita, "40 kHz, 20 ns acousto-optically Q-switched 4 μm Fe:ZnSe laser pumped by a fluoride fiber laser," Opt. Lett. **45**(10), 2788-2791(2020).
15. A. V. Pushkin, E. A. Migal, S. Tokita, Yu. V. Korostelin, and F. V. Potemkin, "Femtosecond graphene mode-locked Fe:ZnSe laser at 4.4 μm," Opt. Lett. **45**(3): 738-741(2020).
16. N. Myoung, V. V. Fedorov, S. B. Mirov, and L. E. Wenger, "Temperature and concentration quenching of mid-IR photoluminescence in iron doped ZnSe and ZnS laser crystals," J. Luminescence **132**, 600-606(2012).
17. A. A.Voronov V. I. Kozlovsky, Yu. V. Korostelin, A. I. Landman, Yu. P. Podmar'kov, Ya. K. Skasyrsky, and M. P. Frolov, "A continuous-wave Fe^{2+}:ZnSe laser," Quantum Electron. **38**(12), 1113-1116(2008).
18. J. W. Evans, T. Sanamyan, and P. A. Berry, "A continuous-wave Fe:ZnSe laser pumped by an efficient $Er:Y_2O_3$ laser," Proc.SPIE **9342**:93420F(2015).
19. D. V. Martyshkin, V. V. Fedorov, M. Mirov, I. Moskalev, S. Vasilyev, V. Smolski, A. Zakrevskiy, and S.B. Mirov, "High Power (9.2 W) CW 4.15 μm Fe:ZnSe laser," CLEO **STh1L6**(2017).
20. E. Li, H. Uehara, W. Yao, S. Tokita, F. Potemkin, and R. Yasuhara, "High-efficiency, continuous-wave Fe:ZnSe mid-IR laser end pumped by an Er:YAP laser," Opt. Express **29**(26), 44118-44128(2021).
21. S. Tokita, M. Murakami, S. Shimizu, M. Hashida, and S. Sakabe, "Liquid-cooled 24 W mid-infrared

Er:ZBLAN fiber laser," Opt. Lett. **34**(20), 3062~3064(2009).

22. V. Fortin, M. Bernier, S. T. BAH, and R. Vallee, "30 W fluoride glass all-fiber laser at 2.94 μm," Opt. Lett. **40**(12), 2882-2885(2015).
23. Y. O. Aydin, V. Fortin, R. Vallee, and M. Bernier, "Towards power scaling of 2.8 μm fiber lasers," Opt. Lett. **43**(18), 4542-4545(2018).
24. A. V. Pushkin, E. A. Migal, H. Uehara, K. Goya, S. Tokita, M. P. Frolov, Yu. V. Korostelin, V. I. Kozlovsky, Ya. K. Skasyrsky, and F. V. Potemkin, "Compact, highly efficient, 2.1-W continuous-wave mid-infrared Fe:ZnSe coherent source, pumped by an Er:ZBLAN fiber laser," Opt. Lett. **43**(24), 5941-5944(2018).
25. S.B. Mirov, I.S. Moskalev, S. Vasilyev, V. Smolski, V.V. Fedorov, D. Martyshkin, J. Peppers, M. Mirov, A. Dergachev and V. Gapontsev, "Frontiers of mid-IR lasers based on transition metal doped chalcogenides". IEEE J. Sel. Top. Quantum Electron., **24**(5),1601829 (2018).
26. J. W. Evans, P. A. Berry, K. L. Schepler, "A broadly tunable continuous-wave Fe:ZnSe laser," Proc.SPIE **8599**, 85990C(2013).
27. V. V. Fedorov, S. B. Mirov, A. Gallian, D. V. Badikov, M. P. Frolov, Yu. V. Korostelin, V. I. Kozlovsky, A. I. Landman, Yu. P. Podmar'kov, V. A. Akimov, and A. A. Voronov, "3.77-5.05-μm tunable solid-state lasers based on Fe^{2+}-doped ZnSe crystals operating at low and room temperatures," IEEE J. Quant. Electron **42**(9), 907-917(2006).
28. X. Zhu, and R.Jian, "Numerical analysis and experimental results of high-power Er/Pr:ZBLAN 2.7 μm fiber lasers with different pumping designs," Appl. Opt. **45**(27), 7118~7125(2006).
29. Evans J W. "Iron-doped zinc selenide: spectroscopy and laser development [D]", Air University, 2014.
30. Q. Pan, F. Chen, J. Xie, C. Wang, Y. He, D. Yu. and K. Zhang, "Theoretical study of the characteristics of a continuous wave iron-doped ZnSe laser," Laser Phys., **28**, 035002(2018).
31. J. Yang;Y. Tang, R. Zhang, and J. Xu, "Modeling and Characteristics of Gain-Switched Diode-Pumped Er-Yb Codoped Fiber Lasers," IEEE J. Quant. Electron 48(12), 1560-1567(2012).
32. H. Cankaya, U. Demirbas, A. K. Erdamar, and A. Sennaroglu, "Absorption saturation analysis of Cr^{2+}:ZnSe and Fe^{2+}:ZnSe," J. Opt. Soc. Am. B, 25(5), 794-800 (2008).